Spatial variability of pyroxenite layers in the Beni Bousera orogenic peridotite (Morocco) and implications for their origin

Kamar Chetouani, Jean-Louis Bodinier, C. J. Garrido, Claudio Marchesi, Isma Amri, Kamal Targuisti

▶ **To cite this version:**

Kamar Chetouani, Jean-Louis Bodinier, C. J. Garrido, Claudio Marchesi, Isma Amri, et al.. Spatial variability of pyroxenite layers in the Beni Bousera orogenic peridotite (Morocco) and implications for their origin. Comptes Rendus Géoscience, 2016, 348 (8), pp.619-629. 10.1016/j.crte.2016.06.001 . hal-01468018

HAL Id: hal-01468018
https://hal.science/hal-01468018

Submitted on 6 Jun 2017

HAL is a multi-disciplinary open access archive for the deposit and dissemination of scientific research documents, whether they are published or not. The documents may come from teaching and research institutions in France or abroad, or from public or private research centers.

L'archive ouverte pluridisciplinaire **HAL**, est destinée au dépôt et à la diffusion de documents scientifiques de niveau recherche, publiés ou non, émanant des établissements d'enseignement et de recherche français ou étrangers, des laboratoires publics ou privés.

C. R. Geoscience 348 (2016) 619–629

Contents lists available at ScienceDirect

Comptes Rendus Geoscience

www.sciencedirect.com

Tectonics, Tectonophysics

Spatial variability of pyroxenite layers in the Beni Bousera orogenic peridotite (Morocco) and implications for their origin

Kamar Chetouani [a], Jean-Louis Bodinier [b,*], Carlos J. Garrido [c], Claudio Marchesi [c,d], Isma Amri [a], Kamal Targuisti [a]

[a] Laboratoire de Géologie de l'Environnement et Ressources Naturelles, Département de Géologie, Université Abdelmalek-Essaâdi, Faculté des Sciences, BP 2121, Tétouan, Morocco
[b] Géosciences Montpellier, Université de Montpellier, CNRS and UA, Campus Triolet, CC 60, Place Eugène-Bataillon, 34095 Montpellier cedex 05, France
[c] Instituto Andaluz de Ciencias de la Tierra (IACT), CSIC and UGR, Avenida de las Palmeras 4, 18100 Armilla, Granada, Spain
[d] Departamento de Mineralogía y Petrología, UGR, Avenida Fuentenueva s/n, 18002 Granada, Spain

ARTICLE INFO

Article history:
Received 27 February 2016
Accepted after revision 7 June 2016
Available online 9 August 2016

Handled by Marguerite Godard

Keywords:
Crustal recycling
Melt–rock reaction
Mantle pyroxenite
Orogenic peridotite
Beni Bousera

ABSTRACT

The Beni Bousera peridotite contains a diversity of pyroxenite layers. Several studies have postulated that at least some of them represent elongated strips of oceanic lithosphere recycled in the convective mantle. Some pyroxenites were, however, ascribed to igneous crystal segregation or melt–rock reactions. To further constrain the origin of these rocks, we collected 171 samples throughout the massif and examined their variability in relation with the tectono-metamorphic domains. A major finding is that all facies showing clear evidence for a crustal origin are concentrated in a narrow corridor of mylonitized peridotites, along the contact with granulitic country rocks. These peculiar facies were most likely incorporated at the mantle–crust boundary during the orogenic events that culminated in the peridotite exhumation. The other pyroxenites derive from a distinct protolith that was ubiquitous in the massif before its exhumation. They were deeply modified by partial melting and melt–rock reactions associated with lithospheric thinning.
© 2016 Académie des sciences. Published by Elsevier Masson SAS. This is an open access article under the CC BY-NC-ND license (http://creativecommons.org/licenses/by-nc-nd/4.0/).

1. Introduction

Orogenic peridotites contain a variety of pyroxene-rich mafic to ultramafic layers, often collectively referred to as 'pyroxenites', although they may also include garnet granulites and eclogites (Bodinier and Godard, 2014). These rocks were given a peculiar attention, with several studies aiming to assess the suggestion by Allègre and Turcotte (1986) that the mafic layers represent elongated strips of oceanic lithosphere recycled in the convective mantle (the 'Marble Cake' model). The Beni Bousera orogenic peridotite, in the Rif mountains of northern Morocco, is well known for containing a wide variety of pyroxenite layers (Kornprobst et al., 1990; Pearson et al., 1989, 1993). A large proportion of the published works supporting a 'Marble Cake' origin for the orogenic pyroxenites are based indeed on samples from Beni Bousera and, to a lesser degree, from the neighbouring Ronda massif, southern Spain (e.g., Allègre and Turcotte, 1986; Kornprobst et al., 1990; Morishita et al., 2003; Pearson and Nowell, 2004). However, several studies of the Beni Bousera pyroxenites also reported evidence for

* Corresponding author.
E-mail address: bodinier@gm.univ-montp2.fr (J.-L. Bodinier).

http://dx.doi.org/10.1016/j.crte.2016.06.001
1631-0713/© 2016 Académie des sciences. Published by Elsevier Masson SAS. This is an open access article under the CC BY-NC-ND license (http://creativecommons.org/licenses/by-nc-nd/4.0/).

igneous garnet crystallisation and suggested that at least part of them originated as high-pressure crystal segregates in magma conduits, variably modified by metamorphic or metasomatic reactions (Gysi et al., 2011; Kornprobst et al., 1990; Pearson et al., 1989, 1993). This interpretation was classically suggested for pyroxenite layers in other orogenic lherzolites (e.g., Bodinier and Godard, 2014).

The different interpretations may partly reflect the diversity of pyroxenite layers in Beni Bousera. The studies supporting the recycling scenario were mostly performed on relatively rare, peculiar rock types including a graphitized diamond-bearing pyroxenite (Pearson et al., 1989) and corundum-bearing aluminous pyroxenites (Kornprobst et al., 1990). Gysi et al. (2011) studied different types of pyroxenites, including more 'classic' garnet pyroxenite layers, collected along two tens of meters long river sections. However, none of the published studies embraces the full range of the pyroxenite variability and the approaches generally do not consider the relationships between pyroxenite layers and the petro-structural variations in host peridotites (Frets et al., 2014). Studies of pyroxenites in the neighbouring Ronda peridotite have shown that their variability is strongly correlated with the peridotite tectono-metamorphic domains (Garrido and Bodinier, 1999). Recent studies in Beni Bousera indicate that the massif underwent an evolution comparable to Ronda, including extreme lithospheric thinning (Frets et al., 2014) and melt–rock interactions involving a subduction component (Gysi et al., 2011). During this evolution, which culminated in thrusting of the peridotite bodies amidst continental crust, the massif may have incorporated varied crustal components, including slab-derived melts possibly crystallized as high-pressure segregates (Pearson et al., 1993) or solid granulite components delaminated from the crust and intermingled with lithospheric peridotites (Gysi et al., 2011).

Therefore, before considering the pyroxenite layers of Beni Bousera and their host peridotites as a case study for the convective 'Marble Cake' mantle, it is essential to assess the effect of lithospheric processes. In this study, we provide an overview of the different pyroxenite facies in the Beni Bousera peridotite based on a large dataset of 171 samples collected throughout the massif. We examine their spatial distribution in relation with the tectono-metamorphic domains recently defined by Frets et al. (2014) and use major and trace elements to constrain their origin. The aim was to determine the extent of the chemical perturbations attributable to the late evolutionary stages of the massif and evaluate the original heterogeneity degree of the Beni Bousera parent body.

2. The Beni Bousera orogenic peridotite

The Beni Bousera peridotite massif crops out in the Septides complex, in the lower internal zones of the Alpine Rif belt, in northern Morocco (Kornprobst, 1974). Foliations and lineations are consistent in peridotites and their crustal host rocks. According to Kornprobst (1974), the peridotite body records a polybaric evolution starting at depths > 150 km. A comparison of the structures in the massif and in the overlying crustal units led Afiri et al. (2011) to propose that the peridotites were exhumed in the footwall of a lithospheric extensional shear zone. Detailed structural and petrological mapping of the massif by Frets et al. (2014) showed that it is composed of four tectono-metamorphic domains with consistent kinematics. From top to bottom, these domains include (Fig. 1): (1) garnet-spinel mylonites, (2) Ariégite subfacies fine-grained porphyroclastic spinel peridotites, (3) Ariégite–Seiland subfacies porphyroclastic spinel peridotites, and (4) Seiland subfacies coarse-porphyroclastic to coarse-granular spinel peridotites. Microstructures and crystal preferred orientations point to deformation dominantly by dislocation creep in all domains, but continuous increase in average olivine grain size indicates decreasing plastic work rates from top to bottom. This evolution in deformation conditions is consistent with the change in synkinematic pressure and temperature conditions, from 900 °C at 2.0 GPa in the garnet-spinel mylonites to 1150 °C at 1.8 GPa in the Seiland domain. A diffuse dunitic-websteritic layering subparallel to the foliation suggests deformation in the presence of melt in the Seiland domain. To account for the consistent kinematics and the tectono-metamorphic evolution, implying a temperature gradient of c. 125 °C km^{-1} preserved across the massif, Frets et al. (2014) proposed that the entire peridotite body was a low-angle shear zone, a few kilometres wide, which accommodated exhumation of the base of the lithosphere from 90 to 60 km depth.

3. Classification, petrography and spatial distribution of pyroxenite layers

Kornprobst et al. (1990) recognized two main types of garnet pyroxenite layers in the Beni Bousera massif. Type I is characterized by relatively low (< 10wt%) and nearly constant Al_2O_3 content in bulk rocks, but variable FeO/MgO ratio (0.1–0.8). In contrast, type II has a narrower range of FeO/MgO values (0.1–0.3) but variable Al_2O_3 content; most samples are more enriched in alumina (up to 15%) than type-I pyroxenites. Type-I layers were considered as high-pressure crystal segregates while type-II layers, which notably include corundum-bearing pyroxenites, were interpreted as metamorphosed oceanic gabbros. Thereafter, Pearson et al. (1993) reported a wide diversity of pyroxenite lithologies but it was Gysi et al. (2011) who first proposed a classification of the Beni Bousera pyroxenite layers aiming to embrace their whole diversity range. The classification proposed here is roughly comparable to that of Gysi et al. (2011) and comprises four main groups. It is, however, based on a larger database of 171 samples collected throughout the massif and examined in thin sections (Fig. 1). Our sampling therefore includes rock facies that were incompletely documented by Gysi et al. (2011), such as the peculiar corundum-bearing pyroxenites studied by Kornprobst et al. (1990). Table 1 in the Supplementary material gives the mineral assemblages of the different groups and sub-groups of our classification and summarizes their main characteristics. Fig. 1 shows the distribution of the pyroxenite groups with respect to the tectono-metamorphic domains defined by Frets et al.

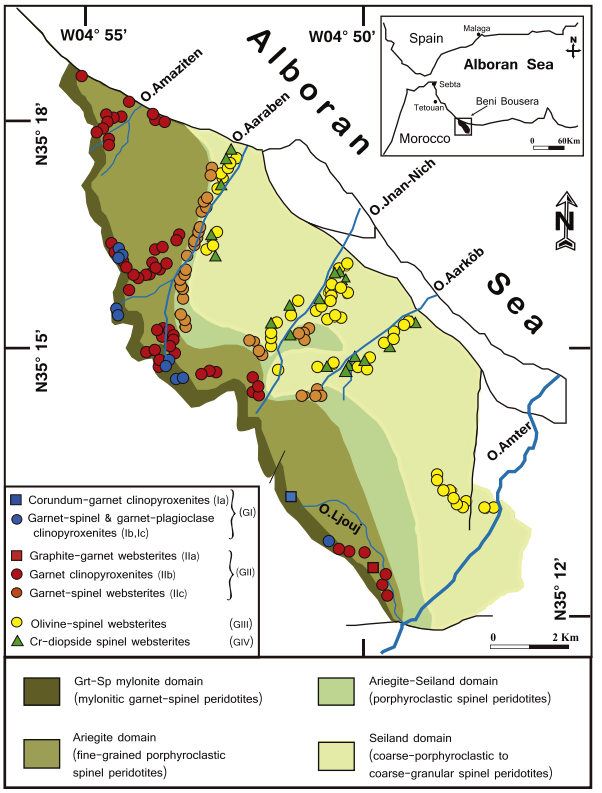

Fig. 1. Geological map of the Beni Bousera peridotite massif showing the tectono-metamorphic domains defined by Frets et al. (2014) and the location of the pyroxenites sampled for this study (see the text and Table 1 for pyroxenite classification). The inset shows the location of the massif in the Alboran realm.

(2014) on the basis of pyroxenite mineralogy and deformation microstructures in peridotites.

Group I: Corundum-garnet (Ia), garnet-spinel (Ib), and garnet-plagioclase (Ic) clinopyroxenites

Group I corresponds to the type-II pyroxenites of Kornprobst et al. (1990). This group also includes the type-IV pyroxenites of Gysi et al. (2011). Group I is composed of pale-grey to greenish, cm- to tens of cm-thick layers occurring exclusively in the Grt–Sp mylonitic domain, along the southwestern border of the massif (Fig. 1). The layers are parallel to the mylonite foliation. They show sharp contacts to the host peridotite, highlighted by narrow rims of bright green Cr-diopside websterite, a few mms to a few centimetres thick. Corundum-garnet (subgroup Ia–Fig. 2a) and garnet-spinel clinopyroxenites (subgroup Ib–Fig. 2b) occur in the core of thick layers ($>$ 10 cm) and grade outwards to garnet-plagioclase ($\pm$ spinel) clinopyroxenites (subgroup Ic). However, several group-I layers, including all thin layers ($<$ 10 cm), are fairly homogeneous and composed only of subgroup-Ic clinopyroxenites (Fig. 2c).

Group-I pyroxenites are distinguished from the other pyroxenites in Beni Bousera by a dominant granoblastic microstructure where large porphyroclasts of clinopyroxene, garnet, corundum and/or Al-spinel are embedded in a mosaic recrystallized matrix of clinopyroxene and garnet, plus variable but generally subordinate amounts of orthopyroxene, plagioclase, spinel, sapphirine, amphibole and olivine (Frets et al., 2012). Clinopyroxene contains up to 20wt% Al_2O_3 combined with a relatively low Na_2O content, resulting in a high proportion of the Ca-Tschermak molecule (Kornprobst et al., 1990). Spinel is green in thin section and contains less than 1wt% Cr_2O_3.

Group II: Graphite-garnet websterites (IIa), garnet clinopyroxenites (IIb), and garnet-spinel websterites (IIc)

Group II corresponds to the type-I pyroxenites of Kornprobst et al. (1990) and the type-III garnet-bearing pyroxenites of Gysi et al. (2011). Group-II pyroxenites are found in the Grt–Sp mylonite, Ariégite subfacies and Ariégite–Seiland subfacies tectonic domains (Fig. 1) where they occur as grey to dark-purplish, cm- to meter-scale layers parallel to the peridotite foliation (Fig. 2e). They show rather sharp contacts with the host peridotite and are commonly isoclinally folded or boudinaged (Fig. 2f). Thinner ($<$ 1 cm) lenses of greenish garnet pyroxenites are also quite common, particularly in mylonites where they were stirred and dispersed by the deformation. Thin layers ($<$ 1 m) may occur in several meters-thick sequences where the pyroxenites volumetrically predominate over the host peridotite. The thicker layers are often zoned, from subgroup-IIb garnet-rich clinopyroxenite in the central part to subgroup-IIc websterite outwards, or from subgroup-IIc in the centre to group-III spinel websterite (below) in the external part. The garnet-graphite websterites (subgroup IIa–Fig. 2d) are a rare rock type (Pearson et al., 1989, 1993), represented by only a couple of thick ($>$ 1 m) layers outcropping in the southwestern part of the massif, close to the contact with granulitic country

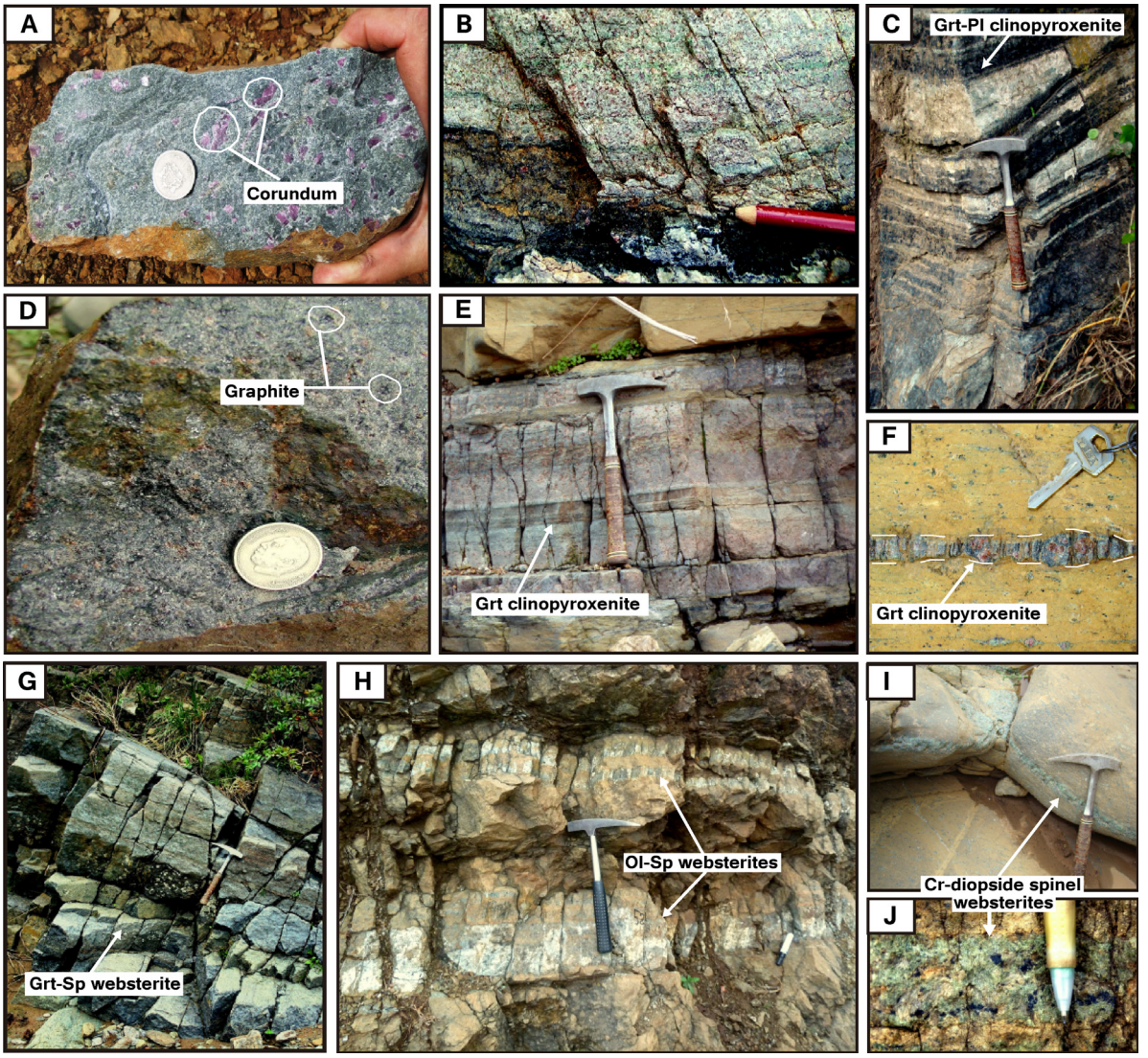

Fig. 2. Photographs of representative samples and field occurrences of the Beni Bousera pyroxenites. A: Subgroup-Ia corundum-garnet clinopyroxenite; B: Subgroup-Ib garnet-spinel clinopyroxenite; C: Subgroup-Ic garnet-plagioclase clinopyroxenite; D: Subgroup-IIa graphite-garnet websterite; E & F: Subgroup-IIb garnet clinopyroxenites; G: Subgroup-IIc garnet-spinel websterite; H: Group-III olivine-spinel websterite; I & J: Group-IV Cr-diopside spinel websterites. See the text and Table 1 for pyroxenite classification.

rocks (Fig. 1). In contrast, the garnet clinopyroxenites (subgroup IIb–Fig. 2e, f) are a common and widespread rock type occurring throughout the Grt–Sp mylonites and the Ariégite peridotite subfacies (Fig. 1). The garnet-spinel websterites (subgroup IIc–Fig. 2g) are specific of the Ariégite–Seiland peridotite subfacies, defined by Frets et al. (2014) as a narrow transition domain between the Ariégite and Seiland domains.

Group-II pyroxenites are characterized by a porphyroclastic microstructure. Coarse garnets (up to 1 cm) are the predominant porphyroclasts in garnet clinopyroxenites (IIb), with only sparse and smaller (1 mm) relicts of clinopyroxene porphyroclasts, whereas the websterites (IIa and IIc) also contain large porphyroclasts of augitic clinopyroxene – up to 2 cm long in subgroup IIc, where they are strongly deformed. Garnet porphyroclasts occur either as isolated grains or as aggregates forming a compositional layering parallel to the foliation. Garnet is either rimmed by kelyphite (IIa and IIb) or deeply kelyphitized (IIc). Kelyphite mineralogy includes orthopyroxene, Al-spinel, amphibole and plagioclase. Clinopyroxene pophyroclasts are rich in exsolutions, particularly in the websterites (IIa and IIb–Gysi et al., 2011). Porphyroclastic minerals are enclosed in a fine-grained matrix (250–300 μm) of recrystallized clinopyroxene and garnet (IIa and IIb) or in a coarser-grained (1 mm) assemblage dominated by ortho- and clinopyroxene (IIc). Subgroup IIa is further distinguished by the presence of a significant amount of graphite (> 15 wt%), containing relict inclusions of micro-diamonds (El Atrassi et al., 2011), and subgroup IIc by the presence of interstitial Cr-spinel.

Group III: Olivine-spinel websterites

Group-III olivine-spinel websterites (= Type-II spinel websterites of Gysi et al., 2011) are characteristic of the Seiland peridotite domain, where they represent the predominant pyroxenite facies (Fig. 1). They occur as greyish to dark-greenish, 2–10 cm thick, single layers (Fig. 2h) or in the centre of composite layers rimmed by group-IV Cr-diopside websterites. They may also be found in the transitional Ariégite–Seiland domain, in the outer part of group-II layers. Group III is primarily distinguished from groups I and II by the lack of garnet and kelyphite whereas aluminous spinel is a major phase (5–10 wt%). Compared with groups I and II, the contacts of group-III pyroxenites to host peridotites are generally more diffuse. This is particularly true in layers characterized by a high proportion (up to 60wt%) of olivine near the contacts, where this mineral occurs as large (~1 cm) crystals elongated parallel to the peridotite foliation.

Group-III microstructure is coarse porphyroclastic. Pyroxenes occur as large, strongly deformed porphyroclasts (up to 2 cm for clinopyroxene) or as virtually undeformed aggregates with holly-leaf shaped spinel, plagioclase and amphibole. The aggregates may be aligned parallel to peridotite foliation and are comparable to the symplectitic aggregates described in the Ronda spinel websterites (type-B of Garrido and Bodinier, 1999) and considered to represent former garnets. Pyroxene porphyroclasts are surrounded by a matrix of medium-sized (0.5–1 mm) anhedral pyroxene neoblasts, and both the porphyroclasts and the medium-grained matrix are further embedded in a very-fine grained matrix that is present in variable proportions.

Group IV: Cr-diopside spinel websterites

Group IV pyroxenites are generally distinguished by greenish to bright-green colours in the field. This group is mostly observed in the Seiland peridotite subfacies (Fig. 1), especially in the lower part of this domain where it is found in association with harzburgites and dunites. Other types of bright-green pyroxenites, sometimes containing garnet, are observed locally in the other peridotite domains where they occur as narrow reaction rims at the contact between garnet pyroxenites and host peridotites. In the Seiland domain, group-IV websterites typically occur as irregularly-shaped lenses and thin veinlets (a few mms to cms thick–Fig. 2i), sometimes forming anastomosed networks crosscutting the peridotite foliation. The contacts are diffuse and the veins may grade into peridotites 'impregnated' by secondary pyroxene and Cr-spinel. Group-IV Cr-diopside websterites also form the outer part of groups-III/IV composite layers and may alternatively occur as single layers parallel to the peridotite foliation and showing sharper contact with peridotite compared with the lenses and veinlets (Fig. 2j). As postulated for similar rock types in Ronda (group D of Garrido and Bodinier, 1999), these latter facies are most likely replacive after group-III pyroxenites.

Group-IV microstructures are coarse granular to porphyroclastic, dominated by relatively large orthopyroxene (0.5–1 cm) and smaller Cr-diopside (1–5 mm) crystals associated with anhedral chromium spinel and olivine. These minerals are surrounded by a finer-grained matrix, where anhedral clinopyroxene and Cr-spinel tend to predominate.

4. Major and trace element chemistry

Fifty pyroxenite samples were selected to represent the different petrological rock types and grinded in an agate mortar for bulk rock analyses (Table 2, Supplementary material). Major elements were analysed by XRF at 'Instituto Andaluz de Ciencias de la Tierra' (Granada), with a sequential spectrometer Bruker S4 Pioneer. Trace-element contents were analysed on a quadrupole HP7700x ICP-MS at Geosciences Montpellier (AETE facility, Montpellier) and on an Agilent 8800 ICP-QMS at IACT (Granada), following the procedure described by Ionov et al. (1992). Accuracy of the ICP-MS analyses can be assessed from the results obtained for the UBN and BIR international rock standards (Table 2).

The analysed samples show a wide range of major-element compositions correlated with the pyroxenite petrological facies and the peridotite tectono-metamorphic domains. This feature is well illustrated by the Ca-Tschermak–forsterite–quartz (CaTs–Fo–Qz) ternary diagram (Fig. 3) showing an extended compositional array from the fertile (high CaTs) group-I clinopyroxenites (Grt–Sp mylonite domain) to the refractory (high Fo and/or En) groups-III and IV websterites (Seiland domain). In detail, the corundum-bearing clinopyroxenite (subgroup Ia) has the highest CaTs content and resembles the 'group-IV pyroxenites' of Gysi et al. (2011), interpreted as metagabbros. Although similar to group I in several respects, the 'mafic garnet granulites' from Ronda (subgroup A1 of Garrido and Bodinier, 1999) are distinguished by more evolved compositions, oversaturated in silica (Fig. 3) and characterized by low *mg-no.* (55–85, compared with 81–89 for

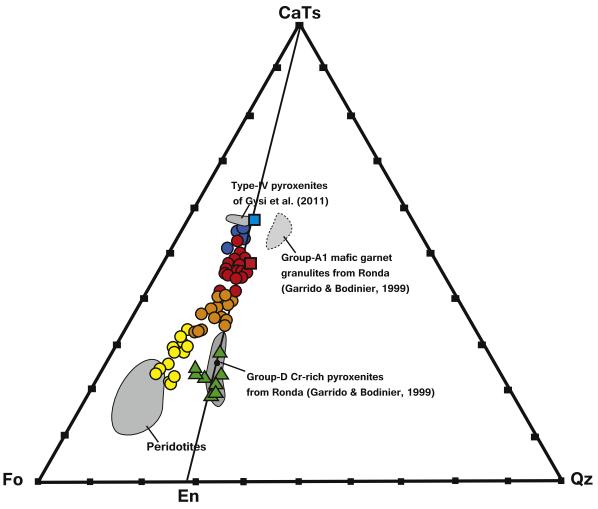

Fig. 3. Molar projections from diopside (Di) into the pseudo-ternary diagram forsterite (Fo)–calcium Tschermak pyroxene (CaTs)–quartz (Qz) of the analysed pyroxenites (symbols for rock types as in Fig. 1), also showing the compositional fields of type-IV pyroxenites from Beni Bousera after Gysi et al. (2011), group-A1 mafic garnet granulites and group-D Cr-rich pyroxenites from Ronda after Garrido and Bodinier (1999), and Beni Bousera peridotites (unpublished data from this study). En: Enstatite.

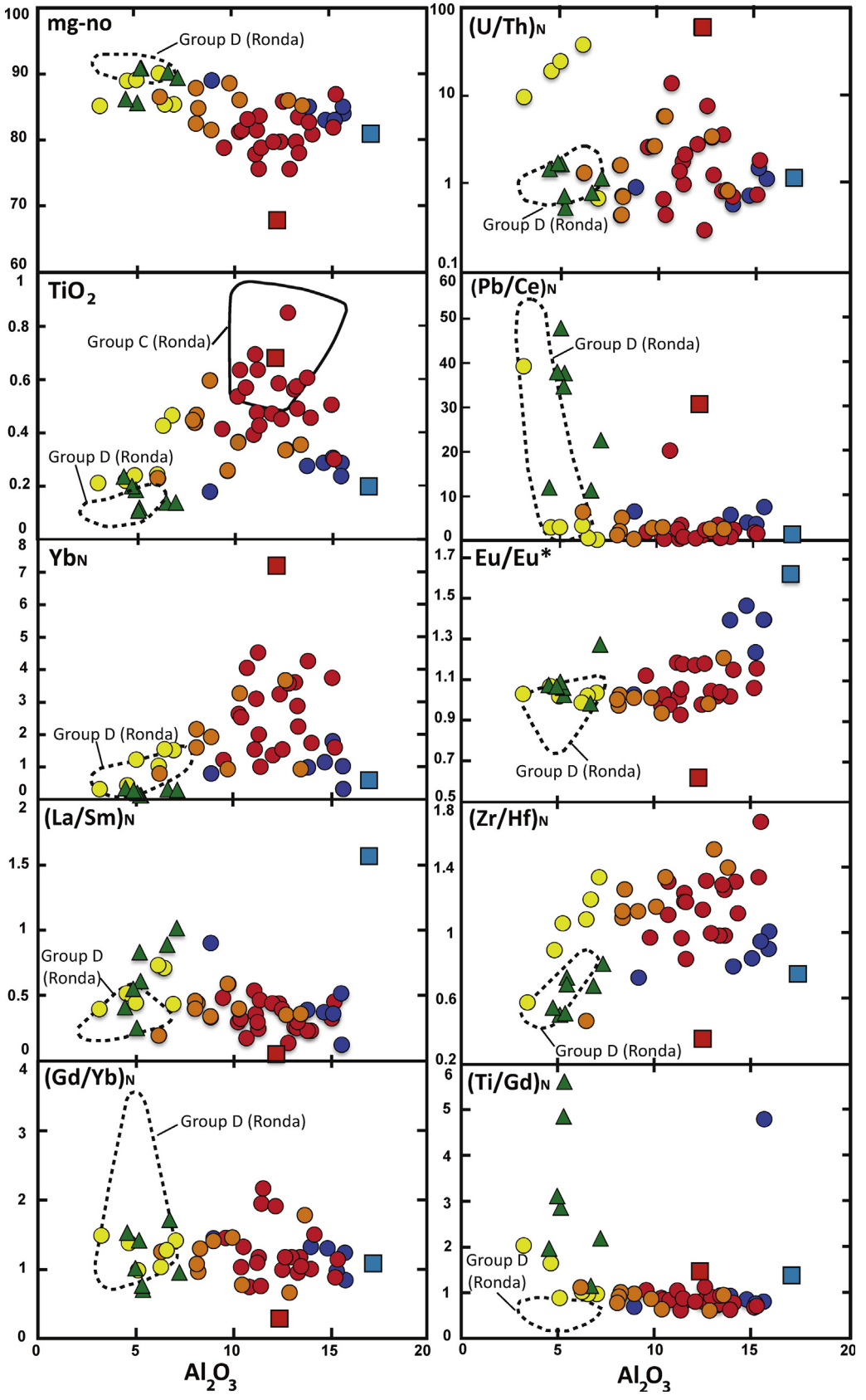
mg-no
Group D (Ronda)
(U/Th)N
Group D (Ronda)
TiO2
Group C (Ronda)
Group D (Ronda)
(Pb/Ce)N
Group D (Ronda)
YbN
Group D (Ronda)
Eu/Eu*
Group D (Ronda)
(La/Sm)N
Group D (Ronda)
(Zr/Hf)N
Group D (Ronda)
(Gd/Yb)N
Group D (Ronda)
(Ti/Gd)N
Group D (Ronda)
Al2O3
Al2O3

group I–Fig. 4). Group-II pyroxenites fill the gap between groups I and groups III–IV, with, however, a clear distinction between subgroups IIa and IIb on one hand (Grt–Sp mylonite and Ariégite domains), and subgroup IIc on the other hand (transitional Ariégite–Seiland domain), the latter being distinctively more refractory. Finally, subgroups III and IV are also well discriminated in Fig. 3: group III is clearly shifted towards the Fo apex and slightly overlaps with peridotite compositions, whereas, similar to their counterparts from the Ronda massif (group-D Cr-rich pyroxenites of Garrido and Bodinier, 1999), the group IV websterites trend towards the En component. A few group-IV samples showing intermediate compositions are likely replacive after group-III websterites.

The *mg-no.*, and the minor and trace elements, are not well correlated with the systematics defined by the major-element components. The *mg-no.* increases with decreasing Al_2O_3 (i.e. with decreasing CaTs/Fo ratio) from groups I and II to groups III and IV (Fig. 4). However, group I is distinguished by higher *mg-no.* values at a given Al_2O_3 content (*mg-no.* = 81–89 in group I, compared with 76–88 in group IIb–c). Conversely, the group-IIa graphite-garnet pyroxenite shows the lowest *mg-no.* (68) in our dataset. TiO_2 and Yb are roughly correlated with Al in groups II and III (Fig. 4), but groups I and IV are distinctively impoverished in these elements, whereas the graphite-garnet websterite (subgroup IIa) is markedly enriched in Yb.

Similar to the majority of pyroxenites from orogenic peridotites (Bodinier and Godard, 2014), most of the analysed samples show chondrite-normalized Rare Earth Elements (REE) patterns similar to N-MORB, i.e. characterized by a rather flat heavy-REE (HREE) segment (Gd–Lu) and depletion in light REE (LREE). In detail, however, the different rock types tend to show distinctive features (Fig. 5):

- as previously noted by Kornprobst et al. (1990) and Gysi et al. (2011), group-I pyroxenites are distinguished by positive Eu anomalies ($Eu/Eu^* > 1.2$–Fig. 4), the highest value (1.6) being observed in the corundum-bearing sample (subgroup Ia);
- Group II is characterized by variable HREE fractionation as illustrated by its wide range of $(Gd/Yb)_N$ values, from 0.3 in the HREE-enriched, graphite-garnet websterite (subgroup IIa) to ~ 2 in some garnet clinopyroxenites (subgroup IIb);
- in addition to being depleted in HREE compared to the other groups, some of group-III and most of group-IV websterites show REE distributions that clearly depart from the 'N-MORB' type, including both convex-upward ('hump-shaped') and somewhat convex-downward ('U-shaped') REE patterns. The latter are observed in the most REE-depleted group-IV samples.

In spite of these variations, the studied pyroxenites show an overall negative correlation between the degree of LREE depletion (La/Sm) and Al_2O_3 (Fig. 4). A notable exception is the corundum-garnet clinopyroxenite (subgroup Ia), which is LREE-enriched. Conversely, the graphite-garnet websterite (subgroup IIa) is strongly depleted in LREE compared with the other group-II pyroxenites (Fig. 5).

The different pyroxenite groups can be fairly well discriminated by a series of selected, Primitive Mantle-normalized inter-element ratios, as illustrated in Figs. 4 and 6:

- Group I is chiefly characterized by high $(Sr/Nd)_N$ values positively correlated with Eu/Eu* (Fig. 6). Like Eu/Eu*, $(Sr/Nd)_N$ shows its highest value (~ 7) in the corundum-bearing sample (subgroup Ia). Compared with the other garnet and garnet-spinel clinopyroxenites (group IIb–c), group I is further distinguished by lower $(Zr/Hf)_N$ (< 1), and higher $(Pb/Ce)_N$ and $(Th/La)_N$ values. The corundum-garnet clinopyroxenite (subgroup Ia) is also distinguished from all the other pyroxenites, except the graphite-garnet websterite (subgroup IIa), by higher, superchondritic Nb/La values ($(Nb/La)_N = 2.4$);
- within group II, the graphite-garnet websterite (subgroup IIa) is clearly distinguished from all the other pyroxenites by elevated $(Nb/La)_N$ and $(U/Th)_N$ ratios (20 and 64, respectively), and very low $(Zr/Hf)_N$ values (0.36) (Figs. 4 and 6). This sample also shows Pb/Ce and Th/La values > PM, well above the values observed in the other group-II pyroxenites. The latter show relatively wide ranges of inter-element ratios, but the values are generally dispersed around PM values (e.g., Pb/Ce), or below in the case of Nb/La and Th/La (Fig. 6);
- Group III is distinguished from group II only by higher U/Th values in several samples (Fig. 4) and the tendency of a few samples to overlap with group-IV websterites for Zr/Hf, Ti/Gd, Pb/Ce, Th/La, and Nb/La;
- Group IV shows several distinctive features, including low, subchondritic Zr/Hf and high, superchondritic Ti/Gd, Pb/Ce, and Th/La ratios. In this respect, group-IV websterites show some similarities with the graphite-garnet websterite (subgroup IIa), in spite of the contrasted mineralogical and major-element compositions of these two rock types (Table 1, Fig. 3), and their well-distinct structural occurrences (Fig. 1).

5. Discussion

Pyroxenite melting and melt–rock reactions

The Beni Bousera pyroxenites show first-order variations of their major-element compositions correlated with pyroxenite petrological facies and peridotite tectono-metamorphic domains (Fig. 3). These variations are reminiscent of the systematics observed in the neighbouring Ronda peridotite (southern Spain), where pyroxenite compositions and rock types are correlated with the major structural domains recognized in the massif (Garrido and Bodinier, 1999). In Ronda, these variations were ascribed to partial melting of the pyroxenites and reaction of residual

Fig. 4. Al_2O_3 (wt.%) covariation diagrams for *mg-no.*, TiO_2 (wt.%), and Primitive Mantle-normalized Yb content and La/Sm, Gd/Yb, U/Th, Pb/Ce, Eu/Eu*, Zr/Hf, and Ti/Gd ratios for the analysed pyroxenites. Fields of group-D Cr-rich pyroxenites and group-C Al-rich pyroxenites from Ronda after Garrido and Bodinier (1999) and Bodinier et al. (2008). *mg.no.* = 100 × Mg/Mg + Fe cationic ratio, with Fe = total iron as Fe^{2+}. $Eu^* = Eu_N/[(Sm_N + Gd_N)/2]$. Normalizing values after McDonough and Sun (1995).

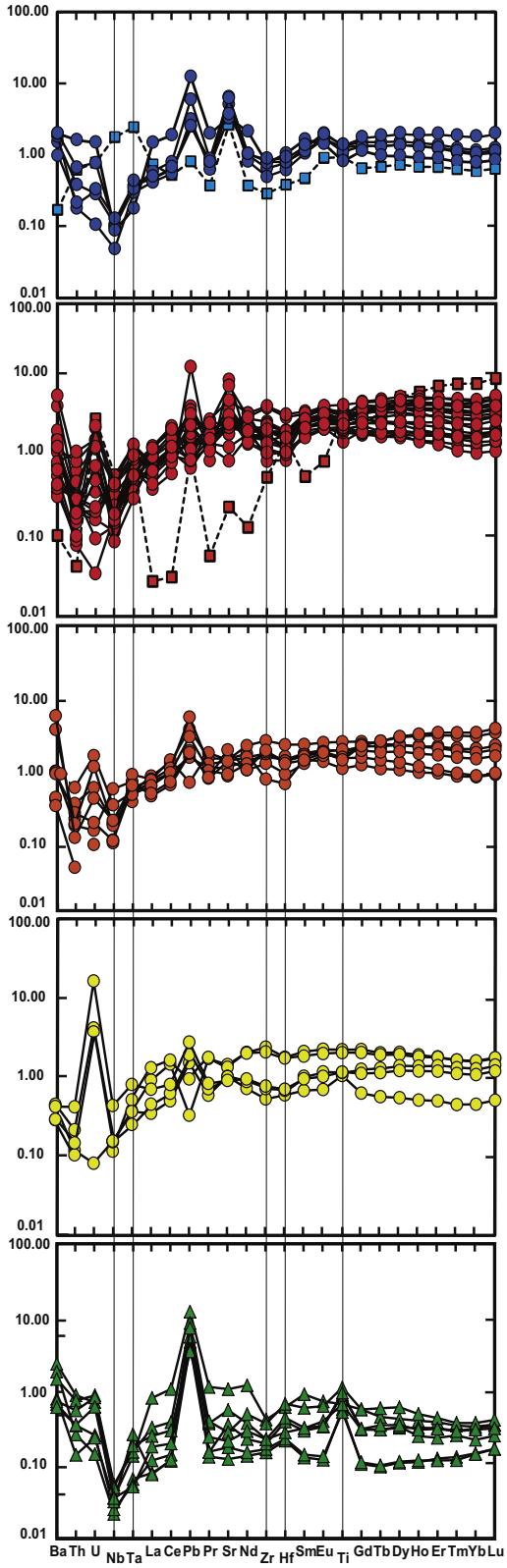

Fig. 5. Chondrite-normalized Rare-Earth Elements (REE) patterns of the analysed pyroxenites (symbols for rock types as in Fig. 1). Normalizing values after McDonough and Sun (1995).

pyroxenites and/or peridotites with peridotite + pyroxenite partial melts, or with subduction-related melts (Bodinier et al., 2008; Garrido and Bodinier, 1999; Lambart et al., 2012; Marchesi et al., 2013). These processes have been ascribed to thinning and heating of subcontinental lithosphere in a back-arc setting, a process that culminated in the massif exhumation (Hidas et al., 2013; Lenoir et al., 2001; Marchesi et al., 2012;). Recently, Frets et al. (2014) proposed extreme lithospheric thinning to explain the tectono-metamorphic zoning of the Beni Bousera massif, and Gysi et al. (2011) suggested the origin (or modification) of certain Beni Bousera pyroxenites as a result of melt infiltration, including subduction-derived melts.

In detail, the major- and trace-element signatures of the studied samples point to three distinct processes involving in-situ or infiltrated partial melts:

(1) the variation from subgroup IIb to subgroup IIc, parallel to the CaTs-En cotectic line and correlated with retrogression of garnet clinopyroxenites (IIb) into garnet-spinel websterites (IIc) can be accounted for by partial melting of a fertile (high CaTs) garnet-clinopyroxenite protolith. Variable HREE fractionation (Figs. 4–5) suggests open-system conditions in the stability field of garnet;

(2) the transition from subgroup IIc to group III and the trend defined by group III towards the peridotite field coincides with compositions experimentally determined by Lambart et al. (2012) for reaction of peridotites with pyroxenite partial melts. This transition marks the boundary between the Ariégite and Seiland peridotite subfacies, and it is worthy of note that in Ronda this boundary coincides with a sharp peridotite melting front (Garrido and Bodinier, 1999). Across the front, major microstructural and chemical changes occur within about 200 m as a result of feedback relationships between crystal growth and partial melting (Lenoir et al., 2001; Van der Wal and Bodinier, 1996). Such a net melting front was not observed in Beni Bousera, but Frets et al. (2012, 2014) noted microstructural changes in peridotites and pyroxenites at the Ariégite–Seiland transition, involving enhanced recrystallization and grain coarsening. Therefore, the offset of group-III olivine-spinel pyroxenites towards the Fo component and peridotite field on figure 3 likely results from reaction of pre-existing group-II pyroxenites (mostly subgroup IIc) with peridotite + pyroxenite partial melts, following the scenario suggested for Ronda spinel pyroxenites by Garrido and Bodinier (1999), Lambart et al. (2012), and Marchesi et al. (2013). Further evidence for generalized melting in the Beni Bousera Seiland domain includes the diffuse contacts between group-III spinel-olivine websterites and their host peridotites, as well as the noticeable abundance of refractory peridotites (harzburgites and dunites) in this domain;

(3) in theory, the composition of group-IV Cr-diopside spinel websterites, which plot close to the En component in figure 3, could reflect interaction of peridotites with a silica-rich melt derived from mafic pyroxenites (Lambart et al., 2012). However, this scenario is

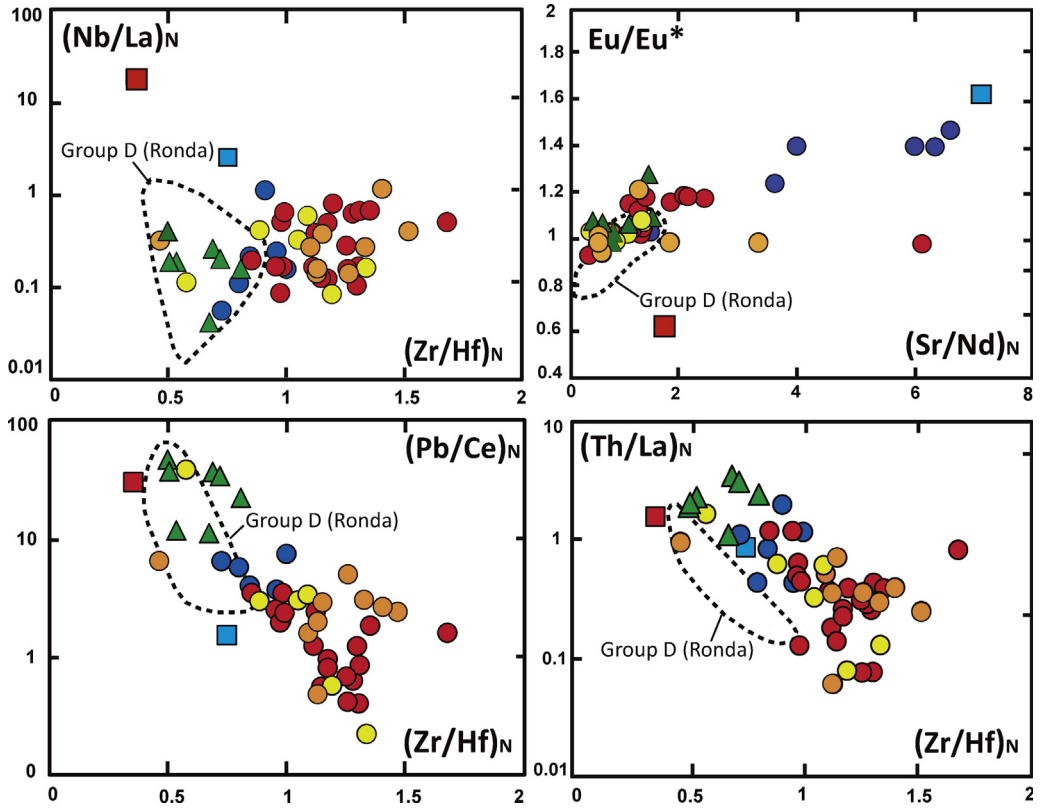

Fig. 6. Primitive Mantle-normalized covariation diagrams for Nb/La, Pb/Ce and Th/La ratios *vs.* Zr/Hf, and Eu/Eu* *vs.* Sr/Nd. Fields of group-D Cr-rich pyroxenites from Ronda after Garrido and Bodinier (1999) and Bodinier et al. (2008). $Eu^* = Eu_N/[(Sm_N + Gd_N)/2]$. Normalizing values after McDonough and Sun (1995).

unlikely because this group is distinguished by a specific trace-element signatures (low Zr/Hf, high Th/La and Pb/Ce ratios - Fig. 6) that is not observed in fertile Beni Bousera pyroxenites, except for the graphite-garnet websterite (subgroup IIa) and, to a lesser degree, for the group-I aluminous pyroxenites. These rock-types occur only in (or very near to) the Grt–Sp mylonite domain, far from the main occurrences of group-IV pyroxenites in the Seiland domain (Fig. 1). As proposed by Gysi et al. (2011), the trace-element signature of group-IV pyroxenites points to infiltration of a subduction-related melt component. Works on similar Cr-rich, pyroxenites from Ronda have suggested their origin by crystal segregation or reactive replacement of pre-existing pyroxenites by refractory melt of boninitic affinity (Garrido and Bodinier, 1999). Cr-rich pyroxenites represent the latest stage of igneous mantle activity, both in Ronda and Beni Bousera, implying that they record a recent evolutionary stage of the massifs in a Cenozoic supra-subduction setting, shortly before their emplacement in the crust (Gysi et al., 2011; Marchesi et al., 2012).

Three distinct pyroxenite protoliths

While pyroxenite melting and melt–rock reactions may account for the first-order major-element systematics observed in the Ca–Ts-Fo–Qz ternary plot (Fig. 3), the *mg-no*, minor- and trace-element systematics (Figs. 4–6) cannot be explained by these processes. Combined together, structural, petrological and geochemical data indicate that the Beni Bousera pyroxenites derive from three different protoliths that were also markedly distinct in terms of relative abundance and spatial distribution:

(1) *Group I* - Based on their fertile composition near the high-CaTs apex in figure 3, group-I pyroxenites might be considered as the ultimate protolith of most Beni Bousera pyroxenites. Since the other pyroxenites show increasing imprint of melting and melt–rock reactions from the Grt–Sp mylonite and Ariégite domains to the Seiland domain, the occurrence of group-I pyroxenites only in the Grt–Sp mylonite domain (Fig. 1) is at first sight consistent with this scenario. However, this hypothesis is ruled out by the *mg-no.*, minor- and trace-element systematics showing that group-II garnet clinopyroxenites cannot derive from group I by partial melting as would be expected in this scheme. As noted above, group I is notably distinguished from group II by higher *mg-no.*, and much lower Ti and HREE contents (Fig. 4). Kornprobst et al. (1990) and Gysi et al. (2011) pointed out the distinctive positive Eu anomalies and Sr enrichments of group-I pyroxenites (Fig. 6), and the implication of this feature for their origin as low-pressure plagioclase-bearing cumulates. Kornprobst et al. (1990), and Morishita et al. (2003) for similar pyroxenites from the Ronda massif, interpreted group-I

pyroxenites as former oceanic crust cumulates recycled in the convective mantle. This hypothesis is, however, at odds with the observation that this particular type of layer is found only in the narrow Grt–Sp mylonite domain, along the contact with granulitic country rocks (Fig. 1). Group I is further distinguished from group II by significantly higher Th/La and Pb/Ce ratios combined with lower Zr/Hf and variable Nb/La values (Fig. 6), suggesting a subduction setting for its origin. Based on their resemblance with island arc cumulates, Gysi et al. (2011) interpreted group-I pyroxenites as delaminated lower arc crust. However, this interpretation does not well account for the concentration of subgroup-Ia, corundum-rich (i.e. former plagioclase-rich) facies in the centre of symmetrically-zoned layers. This feature is suggestive of igneous crystal segregation and the group-I layers may rather represent magmatic sills underplated at the crust–mantle boundary in a supra-subduction setting. In both scenarios, however, they were entrained down to $\geq$60 km depth (Kornprobst et al., 1990), most likely by subduction (see below), before being exhumed back to crustal levels as result of lithospheric thinning (Frets et al., 2014).

(2) *Subgroup IIa* - In addition to the presence of graphitized diamond pseudomorphs (El Atrassi et al., 2011; Pearson et al., 1989, 1993), the graphite-garnet websterite (subgroup IIa) shows several major- and trace-element distinctive features. This sample is the most differentiated in terms of *mg-no.* (Fig. 4) and shows a negative anomaly of Eu (Figs. 4, 5). It is, however, the most LREE-depleted (Fig. 5) and, compared to the other Beni Bousera pyroxenites, is further distinguished by strong enrichments in HREE, Nb-Ta and U, and lower Zr/Hf values. It is also characterized by elevated Pb/Ce and Th/La ratios comparable to the values of group-IV websterites (Figs. 4 and 6). Subgroup-IIa represents therefore a peculiar pyroxenite protolith, likely a high-pressure (garnet- and diamond-bearing) crystal segregate from a partial melt derived from hydrothermally-altered oceanic crust ($\pm$ hemipelagic sediments - Pearson et al., 1991a, b, 1993). However, subgroup IIa, was found only near the contact with crustal granulites, similar to group-I aluminous pyroxenites (Fig. 1). As a consequence, its geochemical signature cannot be used to infer a 'Marble Cake' origin for the whole of the Beni Bousera pyroxenites.

(3) *Subgroup IIb* - The garnet clinopyroxenites occurring throughout the Ariégite and Grt–Sp mylonite domains (subgroup IIb) represent the protolith of subgroup-IIc garnet-spinel websterites, and therefore the ultimate protolith of group-III and replacive group-IV websterites. This implies that subgroup-IIb garnet clinopyroxenites were present throughout the Beni Bousera peridotite at the onset of lithospheric thinning, partial melting and melt–rock reactions that resulted in the individualisation of the different types of pyroxenites observed in the Ariégite–Seiland and Seiland domains (Fig. 1). Kornprobst et al. (1990) suggested an origin of subgroup-IIb garnet clinopyroxenites as high-pressure crystal segregates. However, in contrast with the graphite-garnet websterite (subgroup-IIa), subgroup-IIb garnet clinopyroxenites do not display the systematic HREE enrichment and Zr/Hf fractionation that would be expected in garnet-bearing segregates. Instead, they show geochemical features, notably a high TiO_2 content associated with LREE depletion, that are reminiscent of pyroxenites formed by igneous refertilization (e.g., group C of Ronda after Garrido and Bodinier, 1999 - Fig. 4). A few samples from this subgroup show a subtle positive Eu anomaly associated with slight Sr enrichment (Fig. 6). This may be considered as evidence that their formation involved melting of a recycled, originally plagioclase-bearing source, as proposed by Montanini and Tribuzio (2015) for Ligurian garnet pyroxenites. Subtle anomalies of Eu, either positive or negative, were also observed by Pearson et al. (1991a) in garnet pyroxenites from the Ariégite domain of Beni Bousera. Based on the elevated $\delta^{18}O$ values found in several samples, these authors suggested their crystallization from partial melts of hydrothermally-altered oceanic crust. Similar to other orogenic garnet pyroxenites, subgroup-IIb garnet pyroxenites will clearly deserve further investigations to elucidate the origin of their protolith.

6. Conclusion

Several studies have reported evidence for the Marble Cake model based on the crustal and/or subduction geochemical signatures observed in pyroxenites from the Beni Bousera massif (e.g., Kornprobst et al., 1990; Pearson and Nowell, 2004). Our new trace-element data confirm these early observations. However, these signatures are observed only in peculiar rock types, notably in aluminous garnet clinopyroxenites (group I), including corundum-rich facies (Kornprobst et al., 1990), and in a rare graphite-garnet websterite (subgroup IIa) containing graphitized diamonds (El Atrassi et al., 2011; Pearson et al., 1989, 1993). Most importantly, these rock types are concentrated in a narrow ($<$ 100 m) corridor of mylonitized peridotites, along the contact with the granulitic country rocks. These peculiar facies therefore do not represent recycled components from the convective mantle. They were likely incorporated in the mantle along a major tectonic discontinuity in an early evolutionary stage of the massif, perhaps at the interface between a subducting slab and the overlying mantle wedge. Then this discontinuity would have been re-used during lithospheric thinning, allowing 'recycled', high-pressure pyroxenites to be exhumed along the mantle–crust boundary.

The other types of mafic layers derive from a clearly distinct garnet clinopyroxenite protolith (group IIb) that was ubiquitous in the peridotite body at the onset of lithospheric thinning. However, these layers do not show clear evidence for a crustal or/and subduction origin and thus do not lend support to the Marble Cake model either. Their origin is not fully understood but likely occurred via igneous refertilization mechanisms, as suggested for pyroxenite layering in other orogenic peridotites (Bodinier et al., 2008; Lambart et al., 2012), and possibly involved partial melts from a crustal source (Marchesi et al., 2013; Montanini and Tribuzio, 2015; Pearson et al., 1991a). Thereafter, the original garnet-clinopyroxenite

protolith was deeply modified by partial melting and melt–rock reactions associated with lithospheric thinning. This event probably occurred in a supra-subduction setting (Gysi et al., 2011; Marchesi et al., 2012) and gave rise to a variety of reacted refractory pyroxenites (subgroup IIc, groups III & IV) comparable to those observed in the neighbouring Ronda peridotite (Garrido and Bodinier, 1999).

Acknowledgements

Funding for this study was provided by MAE (France), MESRSFC (Morocco), and CNRS/INSU (France) through the cooperation project #042/STU/09 in the frame of the 'Volubilis Hubert Curien' program (2010–2013) and three INSU research grants ('Actions coordonnées' 2008, and SYSTER 2010 and 2011). C.M. acknowledges funding by Ramón y Cajal Fellowship RYC-2012-11314 by MINECO. This study benefited from the FP7-PEOPLE-2013-IRSES project MEDYNA, funded under Grant Agreement PIRSES-GA-2013-612572, from the International Lithosphere Program CC4-MEDYNA, and from grants funded by the Spanish MINECO (CGL2013-42349-P) and 'Junta de Andalucía' (RNM-131). This research has also benefited from EU Cohesion Policy funds from the European Regional Development Fund (ERDF) and the European Social Fund (ESF). We thank Christophe Nevado (GM) and Rosario Reyes (IACT) for the preparation of samples and high-quality thin sections, and Chantal Douchet (GM) for assistance during ICP-MS analyses. Jean-Marie Dautria is thanked for his help during the petrographic study and Andréa Tommasi for stimulating discussions on the significance of the Beni Bousera mylonite domain. We gratefully acknowledge thorough reviews by Theodoros Ntaflos and Riccardo Tribuzio.

Appendix A. Supplementary data

Supplementary data associated with this article can be found, in the online version, at http://dx.doi.org/10.1016/j.crte.2016.06.001.

References

Afiri, A., Gueydan, F., Pitra, P., Essaifi, A., Précigout, J., 2011. Oligo-Miocene exhumation of the Beni-Bousera peridotite through a lithosphere-scale extensional shear zone. Geodin. Acta 24, 49–60.

Allègre, C.J., Turcotte, D.L., 1986. Implications of a two-component marble-cake mantle. Nature 323, 123–127.

Bodinier, J.-L., Garrido, C.J., Chanefo, I., Bruguier, O., Gervilla, F., 2008. Origin of pyroxenite–peridotite veined mantle by refertilization reactions: evidence from the Ronda peridotite (Southern Spain). J. Petrol. 49, 999–1025.

Bodinier, J.-L., Godard, M., 2014. Orogenic, ophiolitic, and abyssal peridotites. In: Holland, H.D., Turekian, K.K. (Eds.), Treatise on Geochemistry, 2nd edn., vol. 3, Elsevier, Oxford, pp. 103–167.

El Atrassi, F., Brunet, F., Bouybaouène, M., Chopin, C., Chazot, G., 2011. Melting textures and microdiamonds preserved in graphite pseudomorphs from the Beni Bousera peridotite massif, Morocco. Eur. J. Mineral. 23, 157–168.

Frets, E., Tommasi, A., Garrido, C.J., Padron-Navarta, J.A., Amri, I., Targuisti, K., 2012. Deformation processes and rheology of pyroxenites under lithospheric mantle conditions. J. Struct. Geol. 39, 138–157.

Frets, E.C., Tommasi, A., Garrido, C.J., Vauchez, A., Mainprice, D., Targuisti, K., Amri, I., 2014. The Beni Bousera peridotite (Rif Belt, Morocco): and oblique-slip low-angle shear zone thinning the subcontinental lithosphere. J. Petrol. 55, 283–313.

Garrido, C.J., Bodinier, J.-L., 1999. Diversity of mafic rocks in the Ronda peridotite: evidence for pervasive melt/rock reaction during heating of subcontinental lithosphere by upwelling asthenosphere. J. Petrol. 40, 729–754.

Godard, M., Lagabrielle, Y., Alard, O., Harvey, J., 2008. Geochemistry of the highly depleted peridotites drilled at ODP Sites 1272 and 1274 (Fifteen-Twenty Fracture Zone, Mid-Atlantic Ridge): Implications for mantle dynamics beneath a slow spreading ridge. Earth Planet. Sci. Lett. 267, 410–425.

Gysi, A.P., Jagoutz, O., Schmidt, M.W., Targuisti, K., 2011. Petrogenesis of pyroxenites and melt infiltrations in the ultramafic complex of Beni Bousera, northern Morocco. J. Petrol. 52, 1679–1735.

Hidas, K., Booth-Rea, G., Garrido, C.J., Martinez-Martinez, J.M., Padron-Navarta, J.A., Konc, Z., Giaconia, F., Frets, E., Marchesi, C., 2013. Backarc basin inversion and subcontinental mantle emplacement in the crust: kilometre-scale folding and shearing at the base of the proto-Alboran lithospheric mantle (Betic Cordillera, southern Spain). J. Geol. Soc. 170, 47–55.

Ionov, D.A., Savoyant, L., Dupuy, C., 1992. Application of the ICP-MS technique to trace-element analysis of peridotites and their minerals. Geostandards Newsl. 16, 311–315.

Kornprobst, J., 1974. Contribution à l'étude pétrographique et structurale de la zone interne du Rif (Maroc septentrional [Petrography and structure of the Rif inner area, northern Morocco]. Notes Mem. Serv. Geol. Maroc 251, 1–256.

Kornprobst, J., Piboule, M., Roden, M., Tabit, A., 1990. Corundum-bearing garnet clinopyroxenites at Beni Bousera (Morocco): original plagioclase-rich gabbros recrystallized at depth within the mantle? J. Petrol. 31, 717–745.

Lambart, S., Laporte, D., Provost, A., Schiano, P., 2012. Fate of pyroxenite-derived melts in the peridotitic mantle: thermodynamic and experimental constraints. J. Petrol. 53, 451–476.

Lenoir, X., Garrido, C.J., Bodinier, J.-L., Dautria, J.-M., Gervilla, F., 2001. The recrystallization front of the Ronda peridotite: evidence for melting and thermal erosion of subcontinental lithospheric mantle beneath the Alboran basin. J. Petrol. 42, 141–158.

Marchesi, C., Garrido, C.J., Bosch, D., Bodinier, J.-L., Hidas, K., Padron-Navarta, J.A., Gervilla, F., 2012. A Late Oligocene suprasubduction setting in the westernmost Mediterranean revealed by intrusive pyroxenite dikes in the Ronda peridotite (southern Spain). J. Geol. 120, 237–247.

Marchesi, C., Garrido, C.J., Bosch, D., Bodinier, J.-L., Gervilla, F., Hidas, K., 2013. Mantle refertilization by melts of crustal-derived garnet pyroxenite: evidence from the Ronda peridotite massif, southern Spain. Earth Planet. Sci. Lett. 362, 66–75.

McDonough, W.F., Sun, S.S., 1995. The composition of the Earth. Chem. Geol. 120, 223–253.

Montanini, A., Tribuzio, R., 2015. Evolution of recycled crust within the mantle: constraints from the garnet pyroxenites of the External Ligurian ophiolites (northern Apennines, Italy). Geology 43, 911–914.

Morishita, T., Shoji, A., Gervilla, F., Green, D.H., 2003. Closed-system geochemical recycling of crustal materials in alpine-type peridotite. Geochim. Cosmochim. Acta 67, 303–310.

Pearson, D.G., Davies, G.R., Nixon, P.H., 1993. Geochemical constraints on the petrogenesis of diamond facies pyroxenites from Beni Bousera peridotite massif, North Morocco. J. Petrol. 34, 125–172.

Pearson, D.G., Davies, G.R., Nixon, P.H., Greenwood, P.B., Mattey, D.P., 1991a. Oxygen isotope evidence for the origin of pyroxenites in the Beni Bousera peridotite massif, North Morocco: derivation from subducted oceanic lithosphere. Earth Planet. Sci. Lett. 102, 289–301.

Pearson, D.G., Davies, G.R., Nixon, P.H., Mattey, D.P., 1991b. A carbon isotope study of diamond facies pyroxenites and associated rocks from the Beni Bousera peridotite, North Morocco. J. Petrol. 175–189 (special volume: Orogenic lherzolites and mantle processes).

Pearson, D.G., Davies, G.R., Nixon, P.H., Milledge, H.J., 1989. Graphitized diamonds from a peridotite massif in Morocco and implications for anomalous diamond occurrences. Nature 338, 60–62.

Pearson, D.G., Nowell, G.M., 2004. Re-Os and Lu-Hf isotope constraints on the origin and age of pyroxenites from the Beni Bousera peridotite massif: implications for mixed peridotite-pyroxenite mantle sources. J. Petrol. 45, 439–455.

Van der Wal, D., Bodinier, J.-L., 1996. Origin of the recrystallization front in the Ronda peridotite by km-scale pervasive porous melt flow. Contrib. Mineral. Petrol. 122, 387–405.